Floquet Wave Diffraction Theory for Tapered Planar Strip Array Green's Function

F. CAPOLINO

Departimento di Ingegneria dell'Informazione, University of Siena,
Via Roma 56, 53100 Siena-ITALY
e-mail: capolino@dii.unisi.it
Currently, Department of Electrical and Comp. Engineering, University of Houston,
4800 Calhoun Rd., TX 77004, USA
e-mail: macis@ing.unisi.it

F. MARIOTTINI, S. MACI

Departimento di Ingegneria dell'Informazione, University of Siena,
Via Roma 56, 53100 Siena-ITALY

L. B. FELSEN

Department of Aerospace and Mechanical Engineering (part-time),
Boston University, 110 Cummington St., Boston, MA 02215, USA
Also, University Professor Emeritus, Polytechnic University, Brooklyn, NY 11201, USA
e-mail: lfelsen@bu.edu

Abstract

This paper deals with the derivation and physical interpretation of a uniform high frequency representation of the Green's function for a planar phased array of dipoles. The asymptotic representation is based on Floquet wave edge diffraction theory herein extended to accommodate slowly varying tapered amplitude illumination with possible inclusion of dipole amplitudes that tend to zero at the edge. The phased array is assumed to be infinite with uniform amplitude excitation in the z-direction but finite and amplitude-tapered in the x-direction. This geometry permits study of diffraction phenomena occurring at the tapered edge of a rectangular array when the observation point is far from its vertexes, and extends earlier results valid for equiamplitude excitation with inclusion of subdominant slope diffraction terms. Numerical calculations are included to demonstrate the accuracy of the asymptotic algorithm. The results obtained here have already found applications to (i) a Floquet-ray algorithm which is being interfaced with available codes based on the Geometrical Theroy of Diffraction (GTD), and (ii) the construction of a method of moments code which uses global basis functions shaped like diffracted currents arising from the edges and vertexes of the array; both projects are sponsored by the European Space Agency (ESA).

Key Words: *Floquet wave diffraction theory, Fluquet-ray algorithm, array Green's function, truncated large phased arrays, tapered illumination*

1. Introduction

The accurate electromagnetic modeling of large (in terms of the wavelength) finite array antennas is a subject of increasing interest, especially when the antenna operates in a complex electrically large platform environment. Standard ray-tracing techniques applied to each element of the array fail in this case, due to the large number of radiating elements and the hierarchy of interactions with the platform configuration.

The modeling efficiency in such cases is improved substantially if the element-by-element formulation of radiation from a large array antenna is restructured dynamically so as to emphasize its global characteristics as a phased aperture radiator. Relying on similar strategies employed by us previously, the present treatment extends this global reformulation of the array Green's function (AGF) to *tapered* illumination of *truncated* large phased arrays.

In particular, in a sequence of recent papers, an efficient representation of the Green's function for uniformly excited phased arrays has been parameterized in terms of Floquet wave (FW) diffraction theory [1-4] In this framework, the AGF accounts for the collective field radiated by the elementary dipoles through the equivalent radiation from a superposition of continuous FW-matched source distributions windowed over the entire aperture of the array. The asymptotic treatment of the radiation integrals leads to the same FW contributions as those from the infinite structure plus diffracted waves associated with edges and vertexes on the integration domain. This yields a representation which retains the usual convergence advantages of the infinite array FW representation rendering the additional boundary corrections, cast in the format of the Geometrical Theory of Diffraction, computationally very efficient. The resulting algorithm is considerably more convenient than direct summation of the spatial contributions from each element of the array, and it is advantageous for a full-wave analysis of actual arrays structured around the collective AGF [5]. Implementations are presented in [6-8] where the method of moments is constructed around global basis functions shaped like diffracted currents arising from edges and vertexes of the array. Furthermore, the Floquet wave diffraction theory has been interfaced with standard ray-tracing codes as described in [9]. The enormous number of rays emanating from the large number of array elements, and their subsequent interactions with the platform environment, is substantially reduced thereby, since the entire array radiation properties are described in terms of global FWs and their diffraction effects arising from the array truncations. Tracing the relatively few relevant "FW-rays" results in a drastic reduction of computation time.

The truncated FW approach introduced several years ago for one-dimensional [10] and two-dimensional arrays [11, 12] has recently been extended successfully to three-dimensional prototypical configurations via asymptotic isolation of localized diffraction phenomena; e.g., semi-infinite phased dipole arrays located in free space (edge diffraction) [1, 2] or placed on a grounded dielectric slab (edge-excited surface and leaky waves) [13], as well as right-angle sectoral planar phased arrays of dipoles (vertex diffraction) [3, 4]. Time domain analyses of free space configurations have been presented in [14-17].

All cases mentioned above assume equiamplitude excitation and linear phasing; this will be extended here to tapered excitation along one of the array plane coordinates. The reference phased array is assumed to be infinite and uniformly excited in the z-direction but truncated and tapered in the x-direction. The AGF is represented as a plane-wave spectrum in the continuous wavenumber domain (k_x) and in the discrete wavenumber domain $(k_{zq}, \ q = 0, 1, 2...)$ associated with the spatial aperiodic (x) and periodic (z) coordinates, respectively. For each q, we have obtained an efficient and physically incisive uniform asymptotic solution of the spectral integrals, parameterized by their critical spectral points. These spectral points are of two types: i) p-indexed points at which the spectral amplitude function exhibits highly peaked characteristics very similar to those of poles (and therefore denoted by "quasi-poles"), and ii) q-indexed saddle points. The quasi-poles asymptotically define the same FW as the uniformly excited array, with a local amplitude modulation dictated by the tapering function. The steepest descent path asymptotic evaluation at the q-indexed saddle points defines the edge diffracted rays; additional subdominant edge diffracted contributions are introduced to account for slope variation of the tapering function at the edge. The confluence of different types of critical points determines locally uniform transition regions described in terms

of the edge transition function of the Uniform Theory of Diffraction (UTD) [18] and of its "slope diffracted" version [19]. Arrays with tapered excitation have also been analyzed in [20], combining "global" FWs and diffracted fields developed in [1-3] with a numerical technique based on the discrete Fourier transform (DFT). Comparisons between the hybrid DFT-(Floquet ray) algorithm of [20] and the present formulation have been shown in [21] for a tapered strip-array of dipoles. Here, we present the analytic details that were omitted in [21] and some applications to actual array configurations. The paper is organized as follows. In Section 2 the problem is formulated and prepared for successive asymptotics performed in Section 3. In Section 4, numerical examples verify the accuracy and efficiency of the FW-induced asymptotics, also showing to which array antenna problems the theory can be applied. Conclusions are in Section 5.

2.   Formulation

We consider a strip periodic array of linearly phased dipoles located in the x, z-plane of Figure 1a. The array is infinite in the z direction and finite in the x direction, with interelement spatial period along the x and z directions given by d_x and d_z, respectively, and interelement phase gradient γ_x and γ_z, respectively. All dipoles are oriented along the unit vector $\hat{\mathbf{J}}_0$ (a bold character denotes a vector quantity, and a caret ˆ denotes a unit vector). Superimposed upon that background is a x-dependent amplitude tapering function $f(x)$, sampled at the dipole locations,

$$J(nd_x, md_z) = f(nd_x)e^{-j(\gamma_x nd_x + \gamma_z md_z)} \tag{1}$$

with $(x', z') = (nd_x, md_z)$ denoting the location of (m, n)th dipole, and $J(x', z')$ denoting the dipole current amplitude with suppressed time dependence $\exp(j\omega t)$. Without compromising practical utility, we assume $f(x)$ real and positive in the domain $x \in [0, L]$, where $L = (N_x - 1)d_x$ is the dimension of the strip array with N_x dipoles (Figure 1a). The electromagnetic vector field at any observation point $\mathbf{r} = x\hat{\mathbf{x}} + y\hat{\mathbf{y}} + z\hat{\mathbf{z}}$ can be derived from the $\hat{\mathbf{J}}_0$-directed vector potential $A(\mathbf{r})$ by summing over the individual dipole elements

$$A^{tot}(\mathbf{r}) = \sum_{m=-\infty}^{\infty} \sum_{n=0}^{N_x-1} g(\mathbf{r}; nd_x, md_z)f(nd_x)e^{-j(\gamma_x nd_x + \gamma_z md_z)} \tag{2}$$

In (2), $g(\mathbf{r}; nd_x, md_z) = \exp(-jk|\mathbf{R}_{mn}|)/(4\pi|\mathbf{R}_{mn}|)$ with $\mathbf{R}_{mn} = \mathbf{r} - nd_x\hat{\mathbf{x}} - md_z\hat{\mathbf{z}}$ is the free-space scalar Green's function. We employ the k_x, k_z spectral Fourier representation of the free space Green's function [22]

$$g(\mathbf{r}; nd_x, md_z) = \frac{1}{8\pi^2 j} \int_{-\infty}^{\infty} \int_{-\infty}^{\infty} \frac{e^{-j\mathbf{k}\cdot\mathbf{R}_{mn}}}{k_y} dk_x\, dk_z, \tag{3}$$

where

$$\mathbf{k} = k_x\hat{x} \pm k_y\hat{y} + k_z\hat{z}, \quad k_y = \sqrt{k^2 - k_x^2 - k_z^2} \tag{4}$$

and the upper and lower signs apply to $y > 0$ and $y < 0$, respectively. Because of the symmetry, from here on we shall deal with $y > 0$ only. The m-series is summed into closed form via the infinite Poisson sum formula

275
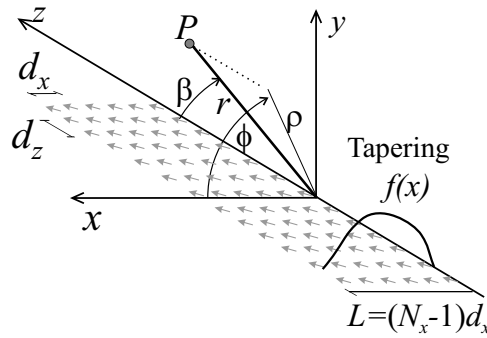
Figure 1. Geometry of the strip array of parallel dipoles oriented along a direction $\hat{u}$. d_x and d_z are the interelement spatial periods along x and z, respectively; N_x is the number of elements along the x direction; $L = (N_x - 1)d_x$ is the dimension of the strip; $f(x)$ is an arbitrary slowly varying tapering.

$$\sum_{m=-\infty}^{\infty} e^{j(k_z - \gamma_z)md_z} = \frac{2\pi}{d_z} \sum_{q=-\infty}^{\infty} \delta(k_z - \gamma_z - \frac{2\pi q}{d_z}) \tag{5}$$

which reduces the k_z integration to a q-series evaluated at the spectral points

$$k_{zq} = \gamma_z + \frac{2\pi q}{d_z}, \quad q = 0, \pm 1, \pm 2, ... \tag{6}$$

Wavenumbers k_{zq} along the untruncated z-domain define the FW dispersion relations. The vector potential A in (2) is thus represented as

$$A^{tot}(\mathbf{r}) = \sum_{q=-\infty}^{\infty} A_q, \tag{7}$$

$$A_q = \frac{e^{-jk_{zq}z}}{4\pi j d_z} \int_{-\infty}^{\infty} I(k_x) \frac{e^{-j(k_x x + k_{yq} y)}}{k_{yq}} dk_x, \tag{8}$$

$$I(k_x) = \sum_{n=0}^{N_x - 1} e^{j(k_x - \gamma_x)nd_x} f(nd_x) \tag{9}$$

where the branch of $k_{yq} = \sqrt{k^2 - k_x^2 - k_{zq}^2}$ is chosen such that $\Im m\, k_{yq} < 0$ on the top Riemann sheet of the k_x-plane. The n-sum $I(k_x)$ in (9) is manipulated via the truncated Poisson sum formula into a p-sum of Fourier transformed f-functions, translated by the FW wavenumbers in the x direction, $k_{xp} = \gamma_x + 2\pi p/d_x$,

$$I(k_x) = \frac{f(0)}{2} + e^{j(k_x - \gamma_x)L} \frac{f(L)}{2} + \frac{1}{d_x} \sum_{p=-\infty}^{\infty} \widetilde{f}(k_x - k_{xp}),$$

$$\widetilde{f}(k_x') = \int_0^L e^{jxk_x'} f(x)dx. \tag{10}$$

in which $\tilde{f}(k'_x)$ is the spectrum of the tapered excitation.

3.   High-Frequency Solution for Slowly Varying $f(x)$

Henceforth, we assume (legitimately for actual tapering functions for large arrays) that $f(x)$ varies slowly with respect to the wavelength λ. Thus, adiabatic methods can be applied, based on perturbation about $f(x) = const.$, which is treated first.

3.1.   Equiamplitude excitation.

Now, the n-series $I(k_x)$ in (10) is evaluated in closed form as

$$I(k_x) = B(k_x)(1 - e^{j(k_x - \gamma_x)L}). \tag{11}$$

with

$$B(k_x) = [1 - e^{jd_x(k_x - \gamma_x)}]^{-1}. \tag{12}$$

Note that the function $I(k_x)$ has no singularities, although $B(k_x)$ has poles at $k_x = k_{xp}$. The semi-infinte array treated in [1] has $I(k_x) = B(k_x)$, which is also obtained from (10) when $N_x \to \infty$. The strip array Green's function can be synthesized from the semi-infinite AGF by omitting the dipole contributions from N_x to ∞; i.e., by subtracting the AGF of a semi-infinite array with spectral shift $\exp(-j(k_x - \gamma_x)L)$ which corresponds to a space translation. For the semi-infinite array, a uniform asymptotic evaluation of (8) is carried out [1] via deformation of the original integration contour into steepest descent paths (SDP) through the saddle points of the phase in the integrand, with extraction of the residues at intercepted poles [1]. The asymptotics is performed through the Pauli-Clemmow regularization [23] and locally uniform evaluation with respect to the pole nearest the saddle point, leading to

$$A^{tot} = \sum_{p,q} A^{FW}_{pq} U(\phi_{pq} - \phi) + \sum_{q} A^d_q, \tag{13}$$

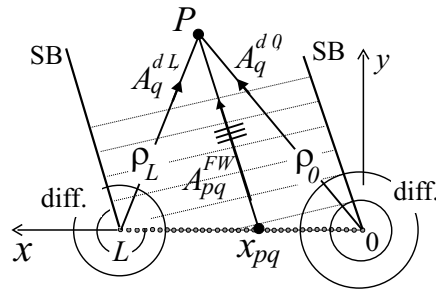$$A^{FW}_{pq} = \frac{e^{-j(k_{xp}x + k_{ypq}y + k_{zq}z)}}{2jd_x d_z k_{ypq}}, \tag{14}$$

$$A^d_q = \frac{e^{-j(k_{\rho q}\rho + k_{zq}z)}}{2d_z\sqrt{2\pi j\rho k_{\rho,q}}} B(k_{x,s})F(\delta^2_{pq}) \tag{15}$$

with $k_{ypq} = \sqrt{k^2 - k^2_{xp} - k^2_{zq}}$ and $k_{\rho,q} = \sqrt{k^2 - k^2_{zq}}$ (branches chosen as in (8)), and cylindrical observation coordinates (ρ, ϕ, z) shown in Figure 1. In (15),

$$F(x) = 2j\sqrt{x}e^{jx} \int_{\sqrt{x}}^{\infty} e^{-jt^2} dt, \ \ \text{with} \ -\frac{3\pi}{2} < arg(x) \le \frac{\pi}{2}. \tag{16}$$

is the standard transition function of the Uniform Theory of Diffraction (UTD) [18], with argument

Figure 2. Wave dynamics in the $x - y$ plane. The p, q-th propagating Floquet wave (FW) exists inside the two p, q-th shadow boundaries (SB), connected to the two edges, and originates at the point $x_{pq} = x - y k_{ypq}/k_{xp}$. Conical diffracted fields arise from the array truncations, their parabolic (in the $x - y$-plane) transition regions are located around the SBs, where they compensate for the FW discontinuity

$$\delta_{pq} = (2 k_{\rho q} \rho)^{-1/2} \sin(\frac{\phi - \phi_{pq}}{2}). \tag{17}$$

It can be shown that when the nondimensional parameter $\delta_{pq}^2 >> 1$, one has $F \to 1$, which reduces the locally uniform diffracted field A_q^d to the nonuniform result away from transition regions. The first series in (13) of FWs arises from the residues at intercepted poles. For a propagating FW, k_{ypq} is real $((k^2 > (k_{xp}^2 + k_{zq}^2))$. For an evanescent FW, k_{ypq} is purely imaginary $((k^2 < (k_{xp}^2 + k_{zq}^2))$, and exhibits exponential decay along y. Therefore, since evanescent FWs in (13) can be neglected without significant loss of accuracy when observing away from the array plane, the $\sum_{p,q}$ is intended only for propagating FWs. In (13), U is the Heaviside unit step function ($U(x) = 1$ or 0 if $x > 0$ or $x < 0$, respectively). The domain of existence of the FW$_{pq}$ is truncated at the shadow boundary (SB) planes $\phi = \phi_{pq}^{SB}$ (see Figure 2) where, for propagating FWs, $\phi_{pq}^{SB} = \phi_{pq} = \cos^{-1}(k_{xp}/k_{\rho q})$. The diffracted field A_q^d in the second series is a conical wave decaying along ρ, discontinuous at the SB planes. Adding this transitional field to that of $A_{pq}^{FW} U(\phi_{pq}^{SB} - \phi)$ restores the continuity of A. Since for $|k_{zq}| > k$, $k_{\rho q} = -j|k_{\rho q}|$, the field A_q^d exhibits exponential decay along ρ. Therefore, since evanescent A_q^d in (13) can be neglected without significant loss of accuracy when observing away from the truncation, $\sum_q$ in (13) then contains only propagating constituents ($|k_{zq}| < k$). Figure 3 shows an example where only two propagating FWs and two propagating diffracted fields arising from the truncation of the array are present. Diffraction cones pertaining to propagating diffracted waves have aperture angles $\beta_q = cos^{-1} k_{zq}/k$ and only those with $q = 0, 1$ are propagating in Figure 3. The physical interpretation of (13) is detailed in [1] and [2].

3.2. Weakly tapered excitation.

With $f(x)$ weakly tapered and positive real in the domain $x \in (0, L)$, the spectrum of $\widetilde{f}(k_x')$ in (10) is localized at $k_x' = 0$, thereby enhancing contributions to $I(k_x)$ from $k_x = k_{xp}$, $p = 0, \pm 1, \dots$ Consequently, the integral in (7) for A_q is dominated asymptotically by a) saddle points (SPs) at $k_x = k_{x,s}$, that satisfy $d/dk_x(k_x x + k_{yq} y)|_{k_{x,s}} = 0$; b) spectral points $k_x = k_{xp}$, that possess the same phenomenology and localization property as the poles for the semi-infinite array, and are therefore called "quasi poles". Uniform
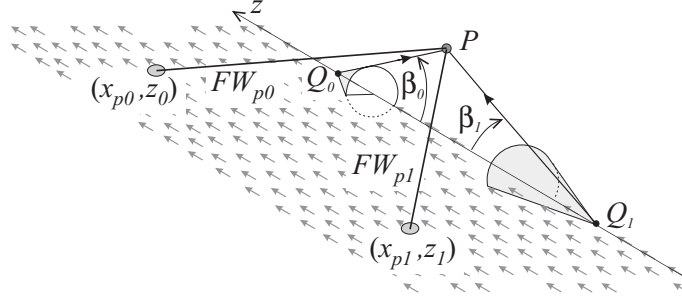
Figure 3. Ray contributions for a planar periodic semi-infinite array. In this particular example, only two propagating FWs and two propagating diffracted-like fields arising from the truncation of the array are present, with $q = 0, 1$. FWs arise from emergence points (x_{pq}, z_q), with $q = 0, 1$. Diffraction cones have aperture angles $\beta_q = \cos^{-1} k_{zq}/k$, with $q = 0, 1$.

evaluation is necessary when a saddle point $k_{x,s}$ approaches one of the k_{xp} "quasi poles" ($p = 0, \pm1, \pm2, ...$). The asymptotic evaluation of A_q is addressed by initially assuming that every k_{xp} is "far enough" from $k_{x,s}$ to validate nonuniform asymptotics. Alternatively, we assume $k_{x,s}$ close to k_{xp}, and obtain a *locally uniform* asymptotic solution, which has been demonstrated to patch onto the nonuniform solution far from the shadow boundary.

3.2.1. Floquet wave contributions.

Inserting (10) into (8), the contributions due to the critical points at $k_x = k_{xp}$ are found by exploring the behavior of the p-th integrand $\widetilde{f}(k_x - k_{xp})e^{-jq(k_x)}k_{yq}^{-1}$ (with $q(k_x) = k_x x + k_{yq}y$) for $k_x \approx k_{xp}$. First we expand the exponent $q(k_x)$ and k_{yq}^{-1} in Taylor series in a neighborhood of $k_x = k_{xp}$,

$$q(k_x) \approx q(k_{xp}) + q'(k_{xp})(k_x - k_{xp}) + \frac{1}{2}q''(k_{xp})(k_x - k_{xp})^2 + ... \tag{18}$$

and

$$k_{yq}^{-1} \approx k_{ypq}^{-1} + k_{xp}k_{ypq}^{-3}(k_x - k_{xp}) + ... \tag{19}$$

Then we extract the phase terms $\exp[-jq(k_{xp}) - jq'(k_{xp})(k_x - k_{xp})]$, with $q(k_{xp}) = k_{xp}x + k_{ypq}y$, and $q'(k_{xp}) = x - k_{xp}y/k_{ypq} = x_{pq}$. Next, we approximate the remaining exponent via the small argument expansion $e^{\xi} \approx 1 + \xi + ...$, leading to

$$\frac{e^{-jq(k_x)}}{k_{yq}} \approx \frac{e^{-j(k_{xp}x+k_{ypq}y)}}{k_{ypq}}e^{-jx_{pq}(k_x - k_{xp})}\left[1 + \frac{k_{xp}}{k_{ypq}^2}(k_x - k_{xp}) + ...\right] \tag{20}$$

which, when inserted into (8), yields

$$A_q' \sim \frac{e^{-jk_{zq}z}}{4\pi jd_xd_z}\sum_{p=-\infty}^{\infty}\frac{e^{-j(k_{xp}x+k_{ypq}y)}}{k_{ypq}}\int_{-\infty}^{\infty}\widetilde{f}(k_x - k_{xp})e^{-jx_{pq}(k_x - k_{xp})}\left[1 + \frac{k_{xp}}{k_{ypq}^2}(k_x - k_{xp}) + ...\right]dk_x \tag{21}$$

279

The contributions due to the first term in parentheses in (21) are calculated directly using the definition of $\tilde{f}(k'_x)$ (see (10)), while those associated to the second term in parentheses are calculated using the derivative $f'(x)$ and the others represent higher order contributions, leading to

$$A'_q \sim \sum_p A^{FW}_{pq} \left[f(x_{pq})U(x_{pq})U(L - x_{pq}) + \frac{jk_{xp}}{k^2_{ypq}} f'(x_{pq})U(x_{pq})U(L - x_{pq}) + ... \right] \tag{22}$$

The pqth FW A^{FW}_{pq} is the same as in (13), but multiplied by the tapering function $f(x_{pq})$ evaluated at the footprint x_{pq} of the pqth FW, shown in Figures 2 and 3. Again, limiting the sum $\sum_p$ to the propagating contributions, x_{pq} is real (because k_{ypq} is real) and the constraint $U(x_{pq})U(L - x_{pq})$ is automatically imposed since $f(x_{pq}) = 0$ for $x_{pq} < 0$ and $x_{pq} > L$ (see Figure 2). In the angular domain, the contributing domain is as in (13) since

$$U(x_{pq}) = U(\phi_{pq} - \phi). \tag{23}$$

Stationary phase evaluation, as in [12], of the radiation integral associated with each p, qth equivalent FW-matched aperture distribution would provide the same result, and in this case, x_{pq} would have been the stationary phase point of the p, qth spatial radiation integral. Criteria for the asymptotic validity of the expansion will be given elsewhere.

3.2.2. FW-modulated diffracted field: nonuniform evaluation.

It will be convenient to find an asymptotic expansion of $I(k_x)$ that highlights the behavior of $f(x)$ at the truncations $x = 0$ and $x = L$. For simplicity we will consider only the end point at $x = 0$. To this end, the FT expression in (10) is inserted into the p-series in $I(k_x)$. The integration is performed by parts as

$$I(k_x) = \frac{f(0)}{2} + e^{j(k_x - \gamma_x)L} \frac{f(L)}{2} + \frac{1}{d_x} \sum_{p=-\infty}^{\infty} \left[\frac{e^{jx(k_x - k_{xp})}}{j(k_x - k_{xp})} f(x) \Big|_0^L - \int_0^L \frac{e^{jx(k_x - k_{xp})}}{j(k_x - k_{xp})} f'(x)dx \right], \tag{24}$$

and can be iterated until the desired asymptotic term. The first term in parentheses provides the first asymptotic diffracted term weighted by the values $f(0)$ and $f(L)$, which the tapering function assumes at the edges. Since in this paper we want to give an accurate evaluation also for weakly illuminated edges, we should include the next iteration of (24), which furnishes a higher order asymptotic term that accounts for the "slope" $f'(0)$ and $f'(L)$ of the tapering at the edges. Using the identities

$$B(k_x) = \frac{1}{2} + \frac{1}{d_x} \sum_{p=-\infty}^{\infty} [-j(k_x - k_{xp})]^{-1}, \tag{25}$$

with $B(k_x)$ defined in (12), and

$$jB'(k_x) = \frac{1}{d_x} \sum_{p=-\infty}^{\infty} [(k_x - k_{xp})]^{-2}, \tag{26}$$

we have

$$I(k_x) \sim [f(0)B(k_x) - jf'(0)B'(k_x)] + +e^{j(k_x-\gamma_x)L}[f(L)B(k_x) - jf'(L)B'(k_x)] + O[(k_x-k_{xp})^{-3}]. \quad (27)$$

The first term is due to the truncation at $x = 0$ while the second term, multiplied by the phase term $\exp(-j(k_x - \gamma_x)L)$, is due to the truncation at $x = L$. Insertion of (27) into (8) yields

$$A_q \sim \frac{e^{-jk_{zq}z}}{4\pi jd_z}\left\{\int_{-\infty}^{\infty}[f(0)B(k_x) - jf'(0)B'(k_x)]\frac{e^{-j(k_xx+k_{yq}y)}}{k_{yq}}\right.$$
$$\left. +\int_{-\infty}^{\infty}[f(L)B(k_x) - jf'(L)B'(k_x)]e^{j(k_x-\gamma_x)L}\frac{e^{-j(k_xx+k_{yq}y)}}{k_{yq}}dk_x\right\}. \quad (28)$$

Diffracted fields arising from the truncations at $x = 0$ and $x = L$ are obtained from saddle points at $k_x = k_{x,s0} = xk_{\rho q}/\rho_0 = k_{\rho q}\cos\phi$ and $k_x = k_{x,sL} = (x-L)k_{\rho q}/\rho_L$, respectively. The transverse distances $\rho_0 = (x^2 + y^2)^{1/2}$, and $\rho_L = ((x-L)^2 + y^2)^{1/2}$ are shown in Figure 2. Saddle point evaluation yields for the nonuniform case

$$A_q^d \sim A_q^{d,0} + A_q^{d,L}, \quad (29)$$

where

$$A_q^{d,0} \sim \frac{e^{-j(k_{zq}z+k_{\rho q}\rho)}}{2d_z\sqrt{2\pi j\rho k_{\rho q}}}[f(0)B(k_{x,s0}) - jf'(0)B'(k_{x,s0}) + ...] \quad (30)$$

is the field arising from the truncation at $x = 0$, and a similar expression holds for the one arising from $x = L$. The dominant asymptotic term (the first in (30)) is the same as that for the uniform case (see (13) with $F \to 1$), except for multiplication by the tapering function evaluated at the edge. The second contribution is of higher asymptotic order since $B(k_x) \equiv \frac{1}{2} + O(k_x^{-1})$ and $B'(k_x) \equiv O(k_x^{-2})$.

Due to phase matching of the various FWs along the z-direction, the point of emergence of the pq-th FW (x_{pq}, z_q) and of the q-th diffracted fields $(0, z_q)$ have the same z-coordinate $z_q = z - k_{zq}\rho/k_{\rho q}$, as shown in Figure 3.

3.3. Uniform representation of the radiated field.

In the vicinity of the shadow boundary (SB) of any propagating FW, nonuniform asymptotics becomes inapplicable due to a) the abrupt emergence or disappearance of any propagating FW across its SB; b) the singularities at the SBs of the nonuniform expression for the diffracted field (we recall that $B(k_x)$ and $B'(k_x)$ have pole singularities of order 1 and 2, repsectively). Uniform asymptotic methods must be invoked in order to ensure smooth compensation of the abrupt emergence or disappearance of any propagating FW across its SB. A locally uniform asymptotic evaluation of the field diffracted from the truncation at $x = 0$ is based on two steps. First, the part containing $B(k_x)$ in the first integral in (28) is evaluated via the saddle point at $k_x = k_{x,s}$ near a critical spectral pole at $k_x = k_{xp}$ as in [1]. The asymptotics is performed through

the Pauli-Clemmow regularization and locally uniform evaluation with respect to the pole nearest the saddle point. The part containing $B'(k_x)$, which has double poles at $k_x = k_{xp}$, is still evaluated in the way shown in [1] but referring instead to a proper canonical integral with a double pole as shown in the Appendix. This leads to a A_q^d diffracted field as in (30) with the inclusion of transition functions.

The total high-frequency solution is

$$A^{tot} = \sum_{pq} f(x_{pq}) A_{pq}^{FW} U(\phi_{pq} - \phi) + \sum_q [A_q^{d,0} + A_q^{d,L}], \tag{31}$$

$$A_q^{d,0} \sim \frac{e^{-j(k_{\rho q}\rho + k_{zq}z)}}{2d_z\sqrt{2\pi j\rho k_{\rho,q}}} \left[f(0)B(k_{xs,0})F(\delta_{pq}^2) - jf'(0)B'(k_{xs,0})F_s(\delta_{pq}^2) \right] \tag{32}$$

were $F(x)$ is the standard UTD transition function defined in (16), and

$$F_s(x) = 2jx[1 - F(x)] \tag{33}$$

is the transition function of the slope diffraction UTD [19]. It can be shown that when the nondimensional parameter $\delta_{pq}^2 >> 1$, $F \to 1$ and $F_s \to 1$, demonstrating that the locally uniform diffracted field A_q^d tends to the nonuniform result in (30) away from transition regions.

3.4.   Total electric vector fields

The vector fields are obtained from the vector potential $\mathbf{A} = A\mathbf{J}_0$, where $\mathbf{J}_0$ represents the direction (unit vector) of the elementary dipoles in the array, via $\mathbf{E} = -j\omega\mu(\mathbf{A} + \nabla\nabla\mathbf{A}/k^2)$, and $\mathbf{H} = \nabla \times \mathbf{A}$. Furthermore, we may consider also an arbitrary planar current on each unit array cell, with spectrum $\mathbf{J}(k_x, k_z)$. When the differential operators are applied to the spectral representation (8), interchanging the order of integration and derivation and noting that the ∇ operator is transformed into $-j\mathbf{k}$ yields

$$\mathbf{E}^{tot} = \sum_{q=-\infty}^{\infty} \mathbf{E}_q \tag{34}$$

$$\mathbf{E}_q = \frac{e^{-jk_{zq}z}}{4\pi d_z} \int_{-\infty}^{\infty} \underline{\mathbf{G}}^E(\mathbf{k}_q)\mathbf{J}(k_x, k_{zq})I(k_x)\frac{e^{-j(k_x x + k_{yq}y)}}{k_{yq}}dk_x, \tag{35}$$

where $\underline{\mathbf{G}}^E(\mathbf{k}) = -\zeta/k(k^2\underline{\mathbf{I}} - \mathbf{k}\mathbf{k})$ is the dyadic electric field spectral Green's function, with $\underline{\mathbf{I}}$ denoting the unit dyadic, and the notation $\mathbf{k}$ in $\underline{\mathbf{G}}^E(\mathbf{k})$ implies a dependence on $(k_x, k_z, k_y(k_x, k_z))$. The magnetic field is formally treated in similar fashion, leading to the replacement of $\underline{\mathbf{G}}^E(\mathbf{k})$ by the magnetic dyadic Green's function $\underline{\mathbf{G}}^H(\mathbf{k}) = -\mathbf{k} \times \underline{\mathbf{I}}$. The asymptotic evaluation of (34) with (35) is carried out in the same way as for the potential A in (8), except that now we shall take into account of the extra term $\underline{\mathbf{G}}^E(\mathbf{k}_q) \cdot \mathbf{J}(k_x, k_{zq})$. The integral (35) is dominated asymptotically by the same spectral points already discussed in Section 3.2: saddle points $k_{x,s0}$ and $k_{x,sL}$, and "quasi poles" at $k_x = k_{xp}$; therefore the procedure is exactly the same outlined in Section 3. Due to the small dimension of the single cell compared to the size of the array, it is legitimate to assume that the spectrum $\mathbf{J}(k_x, k_{zq})$ is slowly varying with respect the phase term and peaks of

$I(k_x)$. Also, the polarization dyadic $\underline{\mathbf{G}}^E(\mathbf{k}_q)$ may be assumed slowly varying. Thus, (35) can be evaluated in a straightforward way as in Section 3, approximating the extra term $\underline{\mathbf{G}}^E(\mathbf{k}_q)\mathbf{J}(k_x, k_{zq})$ at the dominant asymptotic spectral points,

$$\mathbf{E}^{tot} = \sum_{p,q} f(x_{pq})\mathbf{E}_{pq}^{FW} U(\phi_{pq} - \phi) + \sum_q \left[\mathbf{E}_q^{d,0} + \mathbf{E}_q^{d,L}\right] \tag{36}$$

with

$$\mathbf{E}_{pq}^{FW} = \frac{e^{-j(k_{xp}x + k_{ypq}y + k_{zq}z)}}{2d_x d_z k_{ypq}} \underline{\mathbf{G}}^E(\mathbf{k}_{pq}^{FW})\mathbf{J}(k_{xp}, k_{zq}), \tag{37}$$

and

$$\mathbf{E}_q^{d,0} \sim \frac{e^{-j(k_{\rho q}\rho + k_{zq}z)}}{2d_z\sqrt{2\pi j\rho k_{\rho,q}}}\underline{\mathbf{G}}^E(\mathbf{k}_q^{d,0})\mathbf{J}(k_{xs,0}, k_{zq}) \cdot \left[f(0)B(k_{x,s0})F(\delta_{pq}^2) - jf'(0)B'(k_{x,s0})F_s(\delta_{pq}^2)\right] \tag{38}$$

with FW and diffracted field wavenumbers given by $\mathbf{k}_{pq}^{FW} = (k_{xp}, k_{ypq}, k_{zq})$ and $\mathbf{k}_q^{d,0} = (k_{\rho q}\cos\phi, k_{\rho q}\sin\phi, k_{zq})$, respectively, and $k_{x,s0} = k_{\rho q}\cos\phi$. The reader is referred to [1],[2],[3] for more details about the asymptotics involving vector fields.

4.   Illustrative Examples

In Figure 4, the spectrum $I(k_x)$, defined in (9), is plotted for the irreducible spectral zone $-\pi/d_x < k_x < \pi/d_x$, for a particular test array with $N_x = 50$, phasing $\gamma_x = 1.1/\lambda$ and spacing $d_x = \lambda/2$, and with tapering $f(x) = \sin(\pi x/L)$ along the x-direction. Since $I(k_x)$ is periodic with period $2\pi/d_x$, it assumes the same values shown in the plot for k_x outside the irreducible region. The visible region of the q-th term in (8) is defined as $-k_{\rho q} < k_x < k_{\rho q}$. Both saddle points and poles in this region give rise to propagating wave contributions. Only for $q = 0$, $\gamma_z = 0$, $d_x = \lambda/2$, the visible region corresponds with the irreducible zone in the plot. The spectrum $I(k_x)$ is localized at $k_x = k_{xp}$, $p = 0, \pm 1, ...$, and thus at $k_x = k_{x0} = \gamma_x$ in the irreducible zone. Assuming $\gamma_x = 1.1/\lambda$ and $d_x = \lambda/2$ (Figure 4), the peak is at $k_x = 0.175\pi/d_x$, and its sharpness justifies the approximations introduced in (18)-(21) based on the "quasi pole" localization. In this particular case, there is only the "quasi pole" at $k_x = k_{x0}$ in the visible region, and thus only one propagating FW.

4.1.   Array of dipoles

Results in Figure 5 show the accuracy of the truncated Floquet wave (TFW) asymptotics in (36),(38), with inclusion of the diffracted field arising from the truncation at $x = L$, when compared with a reference solution obtained by an element-by-element summation over the radiation due to each dipole. The test array has $N_x = 50$ elements in the x-direction (as in Figure 4) and 2000 elements in the z-direction, so that contributions from x-directed edges and from the corners are negligible. The dipoles are directed along
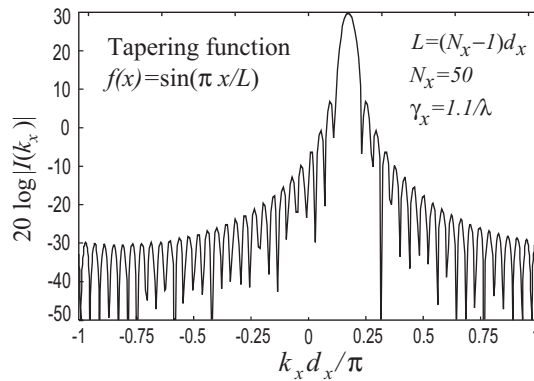
Figure 4. Spectrum $I(k_x)$ in the irreducible range $-\pi/d_x < k_x < \pi/d_x$. We recall that $I(k_x)$ is a periodic function of period $2\pi/d_x$. The visible region of the q-th term in (8) is defined as $-k_{\rho q} < k_x < k_{\rho q}$ which, in the case of $q = 0$, $\gamma_z = 0$, $d_x = \lambda/2$, corresponds with the k_x-range in the plot. The spectrum $I(k_x)$ is localized at $k_x = k_{xp}$, $p = 0, \pm 1, ...$, and thus at $k_x = k_{x0} = \gamma_x$ in the irreducible zone. Assuming $\gamma_x = 1.1/\lambda$ and $d_x = \lambda/2$, the peak is at $k_x = 0.175\pi/d_x$.
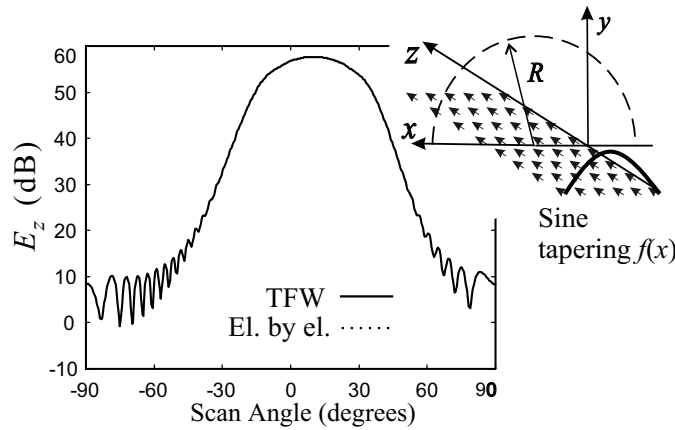

Figure 5. E_z component of the electric field at a distance $R = 20\lambda$ from the center of the array $(x = L/2)$. along a scan in the x, y plane at $z = 0$. Sine excitation.

z, with interelement spacings $d_x = d_z = 0.5\lambda$, interelement phasings $\gamma_z = 0$ and $\gamma_x = 1.1/\lambda$ (beam angle= $10°$ in the x, y plane), and tapering $f(x) = \sin(\pi x/L)$. The E_z component of the electric field is shown in Figure 5 along a scan at $R = 20\lambda$ from the center of the array (at $x = L/2$). Element-by-element and asymptotic results are coincident on the scale of the plot. It is important to note that in this particular case, $f(0) = f(L) = 0$; thus the diffracted field in (38) is given only by the term with $f'(0) \neq 0$, thereby representing a good test case for the additional "slope diffracted field".

4.2. Array of apertures

In order to show the applicability of the above method to actual cases, let us consider a strip-array of z-directed resonant slots ($a \approx \lambda/2$, $b << a$) on an infinite ground plane as shown in Figure 6. The test array (24 elements along x and 600 along z, $d_x = d_z = 0.7\lambda$, $\gamma_x = 1.1\lambda^{-1}$, i.e., beam tilt of $10°$ in the E-plane) is chosen to simulate typical dimensions of a X-band synthetic aperture radar (SAR) antenna (12x0.6 m at
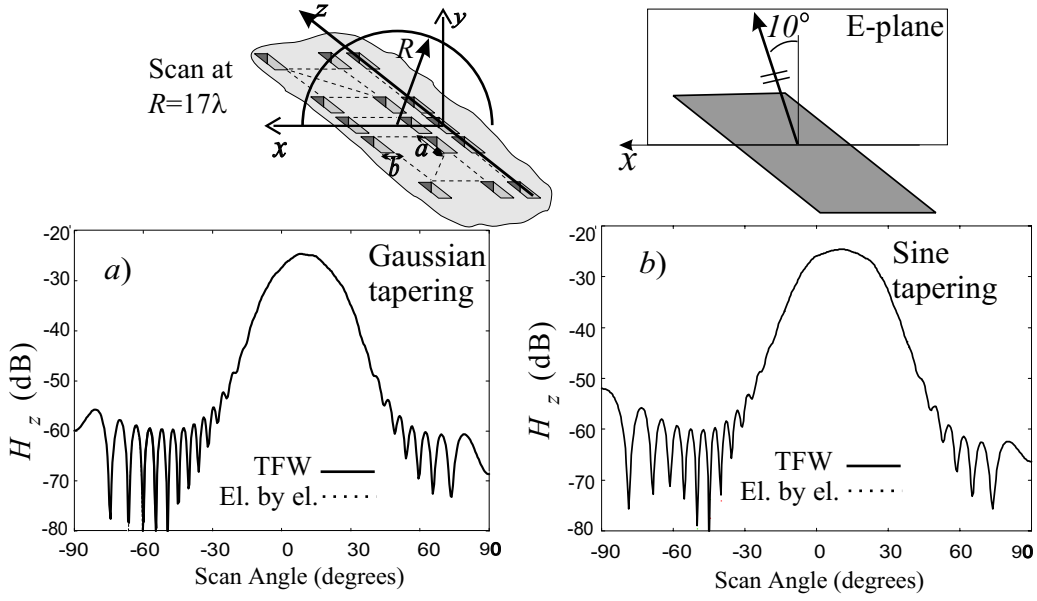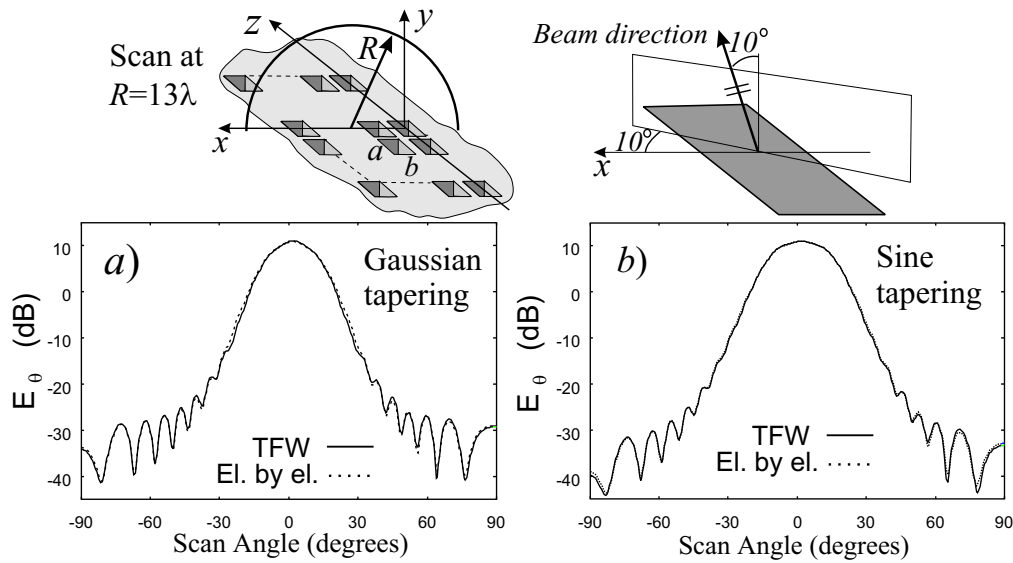
Figure 6. H_z component of the magnetic field radiated by a slot array antenna, at a distance $R = 17\lambda$ from the center of the array $(x = L/2)$. (a) Gaussian excitation; (b) Sine excitation

10GHz). For such dimensions, contributions from x-directed edges and corners are negligible along the scan. The results are calculated via the TFW asymptotics in (36)-(38), with inclusion of the diffracted field arising from the truncation at $x = L$, and compared with a reference solution obtained by an element-by-element summation over the radiation due to each slot. Two cases of $f(x)$ tapering functions are considered: a Gaussian profile $f(x) = \exp(-0.9[(x - L/2)/L]^2)$ with 10% edge illumination (Figure 6a), and a sine profile $f(x) = \sin(\pi x/L)$ (Figure 6b). As in Figure 5, $f(0) = f(L) = 0$ here; and the slope diffracted field is the dominant contributor.

In contrast to the example in Figure 5, the antennas are now modeled as apertures of equivalent magnetic current distributions, and the FW-dipole-excited theory is modified accordingly. The spectrum of the equivalent magnetic currents is assumed as $\tilde{M}(k_z) = (2\pi/a)[\cos(k_z a/2)/[(\pi/a)^2 - k_z^2]$ which determines also the element pattern. Only the H_z component is shown in Figure 6 along a scan at $R = 17\lambda$ from the center of the array $(x = L/2)$. Element-by-element and asymptotic results are not distinguishable on the scale of the plot.

In the last example shown in Figure 7 we consider a test array composed of open-ended wave guides on an infinite ground plane, with $a = 0.57\lambda$, $b = 0.25\lambda$ and with a TE_{10} electric field distribution and major axis along z. We consider a strip-array of 30 elements along x and 1000 along z, $d_x = 0.4\lambda$, $d_z = 0.7\lambda$, for which the beam is tilted $10°$ off the y axis and $10°$ in azimuth from the x axis (see the inset), i.e., $\gamma_x = .19\lambda^{-1}$ and $\gamma_z = 1.07\lambda^{-1}$. For these array dimensions, contributions from the x-directed edges and corners are again negligible and all previous considerations apply. The spectrum of the equivalent magnetic currents is now assumed as $\tilde{M}(k_x, k_z) = 4(ab)^{-1}[\sin(k_x b/2)/k_x][\pi \cos(k_z b/2)/((\pi/a)^2 - k_z^2)]$. Again, element-by-element and asymptotic solutions are in very good agreement.

285

Figure 7. E_θ component of the electric field radiated by an array of aperture antennas, at a distance $R = 13\lambda$ from the center of the array ($L = 17\lambda$). (a) Gaussian excitation; (b) Sine excitation

5. Conclusions

A uniform high frequency representation based on Floquet wave edge diffraction theory has been derived for the Green's function of a planar, nonuniformly excited phased array of dipoles. The slowly varying amplitude tapering along one dimension treated here is introductory for a more complete two-dimensional tapering analysis, which is the topic of a forthcoming paper; however, the one-dimensional tapering case may itself have practical validity for describing diffraction phenomena occurring at a tapered edge of a rectangular array when the observation point is far from its vertexes. The high-frequency representation presented here complements earlier results for equiamplitude excitation through inclusion of slope diffraction contributions, which permits accurate description of the diffraction processes also when the tapered excitation tends to zero at the array edges. These slope diffraction contributions are cast in the format of the slope diffraction UTD [19] for convenient implementation. The uniform asymptotics presented here is physically appealing, numerically accurate, and efficient, owing to the rapid convergence of both the FW series and the series of corresponding FW-excited diffracted fields away from the array plane. These asymptotic constructs have already been combined with available ray-tracer codes [9] to analyze the array performance in the presence of complex platforms. Instead of launching rays from each array element (or group of elements), only a few rays (associated with propagating FWs and their diffracted fields) are traced in the complex environment. The results obtained also provide the basic guidelines for the formulation of a hybrid method where FW-modulated diffracted rays are used as basis functions in a Method of Moment scheme [6,7].

Acknowledgements

Appendix

The standard Fresnel transition functions $F(x)$ and $F_s(x)$ of the UTD [18] and of the slope diffracted UTD [19], respectively, are defined as

$$F(x) = 2j\sqrt{x}e^{jx} \int_{\sqrt{x}}^{\infty} e^{-jt^2} dt, \tag{39}$$

and

$$F_s(x) = 2jx[1 - F(x)] \tag{40}$$

where the argument of the square root, evaluated through its principal value, is defined in the range $-\frac{3\pi}{2} < arg(x) \le \frac{\pi}{2}$. The two transition functions are related one to the other by

$$\frac{d}{d\xi}\frac{F(\xi^2)}{\xi} = -\frac{F_s(\xi^2)}{\xi^2} \tag{41}$$

which can be derived through direct differentiation of the right hand side of (39). As shown in [22, pp.402] and in [1, Eqs.(31)-(33)] the function F usefully describes a canonical integral with quadratic exponent and a single simple pole

$$\int_{-\infty}^{\infty} \frac{e^{-Ks^2}}{s-y} ds = -\sqrt{\frac{\pi}{K}}\frac{F(jKy^2)}{y}. \tag{42}$$

From (42) one may derive the identity

$$\int_{-\infty}^{\infty} \frac{e^{-Ks^2}}{(s-y)^2} ds = \frac{d}{dy}\int_{-\infty}^{\infty} \frac{e^{-Ks^2}}{s-y} ds = -\sqrt{\frac{\pi}{K}}\frac{d}{dy}\frac{F(jKy^2)}{y} \tag{43}$$

which, when combined with (41), leads to

$$\int_{-\infty}^{\infty} \frac{e^{-Ks^2}}{(s-y)^2} ds = \sqrt{\frac{\pi}{K}}\frac{F_s(jKy^2)}{y^2} \tag{44}$$

Introducing the change of variable $x = jKy^2$ in (44) yields

$$\frac{x}{jK}\sqrt{\frac{K}{\pi}} \int_{-\infty}^{\infty} \frac{e^{-Ks^2}}{(s-\sqrt{\frac{x}{jK}})^2} ds = F_s(x) \tag{45}$$

which relates the canonical integral with a double (2nd order) pole and a quadratic exponent to the UTD slope transition function, and has been used for deriving (32) from (28) in Section 3.3.

References

[1] F. Capolino, M. Albani, S. Maci, and L.B. Felsen, "Frequency domain Green's function for a planar periodic semi-infinite dipole array. Part I: Truncated Floquet wave formulation," *IEEE Trans. Antennas Propagat.*, vol. 48, no. 1, pp. 67–74, January 2000.

[2] F. Capolino M. Albani S. Maci and L.B. Felsen, "Frequency domain Green's function for a planar periodic semi-infinite dipole array. Part II: Phenomenology of diffracted waves," *IEEE Trans. Antennas Propagat.*, vol. 48, no. 1, pp. 75–85, January 2000.

[3] F. Capolino S. Maci and L. B. Felsen, "Asymptotic high-frequency Green's function for a planar phased sectoral array of dipoles," *Radio Science-Invited Paper*, vol. 35, no. 2, pp. 579–593, March-April 2000, Ser. Special Issue 1998 URSI Int. Symp. Electromagn. Theory.

[4] S. Maci F. Capolino and L. B. Felsen, "Three dimensional Green's function for planar rectangular phased dipole arrays," *Wave Motion-Invited Paper, Special Issue on Electrodynamics in Complex Environments*, Vol. 34, no.3, pp.263-279, Sept. 2001.

[5] A. K. Skrivervik and J.R. Mosig, "Finite planed array of microstrip patch antennas: the infinite array approach," *IEEE Trans. Antennas Propagat.*, vol. 40, no. 5, pp. 579–582, May 1992.

[6] A. Neto, S. Maci, G. Vecchi, and M. Sabbadini, "Truncated Floquet wave diffraction method for the full wave analysis of large phased arrays. Part I: Basic principles and 2D case.," *IEEE Trans. Antennas Propagat.*, vol. 48, no. 3, pp.594-600, April 2000.

[7] A. Neto, S. Maci, G. Vecchi, and M. Sabbadini, "Truncated Floquet wave diffraction method for the full wave analysis of large phased arrays. Part II: Generalization to the 3D case," *IEEE Trans. Antennas Propagat.*, vol. 48, no. 3, pp.600-611, April 2000.

[8] Ö. A. Çivi, P.H. Pathak, H-T. Chou,and P. Nepa, "A hybrid UTD-MoM for efficient analysis for radiation/scattering from large finite planar arrays," *Radio Science-Invited Paper*, vol. 35, no. 2, PP.607-620, March-April 2000, Ser. Special Issue 1998 URSI Int. Symp. Electromagn. Theory.

[9] F. Capolino, S. Maci, M. Sabbadini and L. B. Felsen, "Large phased arrays on complex platforms," in *ICEAA (Int. Conf. Electromagnetics and Advanced Appl.)*, Torino, Italy, September 10-14 2001.

[10] P-S. Kildal, "Diffraction corrections to the cylindrical wave radiated by a linear array feed of a cylindrical reflector antenna," *IEEE Trans. Antennas Propagat.*, vol. 32, pp. 1111–1116, 1984.

[11] L. Carin and L.B. Felsen, "Time harmonic and transient scattering by finite periodic flat strip arrays: Hybrid (ray)-(Floquet mode)-(MoM) algorithm," *IEEE Trans. Antennas Propagat.*, vol. 41, no. 4, pp. 412–421, April 1993.

[12] L.B. Felsen and L. Carin, "Diffraction theory of frequency- and time-domain scattering by weakly aperiodic truncated thin-wire gratings," *J. Opt. Soc. Am. A*, vol. 11, no. 4, pp. 1291–1306, April 1994.

[13] S. Maci, A. Polemi, A. Toccafoondi and L. B. Felsen, *IEEE Trans. Antennas Propagat.*, vol. 49, no. 12, December 2001.

[14] L. B. Felsen and F. Capolino, "Time domain Green's function for an infinite sequentially excited periodic line array of dipoles," *IEEE Trans. Antennas Propagat.*, vol. 48, no. 6, pp. 921–931, June 2000.

[15] F. Capolino and L. B. Felsen, "Frequency and time domain Green's functions for a phased semi-infinite periodic line array of dipoles," *IEEE Trans. Antennas Propagat.*, vol. 50, January 2002,

[16] F. Capolino and L. B. Felsen, "Time Domain Green's Functions for an Infinite Sequentially Excited Periodic Planar Array of Dipoles," *IEEE Trans. Antennas Propagat.*, vol. 50, 2002, In Print.

[17] F. Capolino and L. B. Felsen, "Short-Pulse Radiation by a Sequentially Excited Semi-infinite Periodic Planar Array of Dipoles," Submitted to *Radio Science-Invited Paper*, Nov. 2001, Ser. Special Issue 2001 URSI Int. Symp. Electromagn. Theory.

[18] R. G. Kouyoumjian and P. H. Pathak, "A uniform geometrical theory of diffraction for an edge in a perfectly conducting surface," *Proc. IEEE*, vol. 62, no. 11, pp. 1448–1461, November 1974.

[19] R. G. Kouyoumjian, "The geometrical theory of diffraction and its applications," *in Numerical and Asymptotic Techniques in Electromagnetics*, 1975, ed. by R. Mittra, Springer-Verlag, New York.

[20] P. Nepa, P.H. Pathak, Ö. A. Çivi, H-T. Chou, "A DFT based UTD ray analysis of the EM radiation from elettrically large antenna arrays with tapered distribution," in *IEEE AP-S/URSI Symposium*, Orlando, FL, July 11-16 1999, p. 85.

[21] F. Capolino, S. Maci and L. B. Felsen, "Floquet wave diffraction theory for tapered planar array Green's functions," in *AP2000 Millennium Conf. Ant. Propagat.*, Davos, Switzerland, April 9-14 2000.

[22] L. B. Felsen and N. Marcuvitz, *Radiation and Scattering of Waves*, Prentice-Hall, Englewood Cliffs, NJ, 1973. Also IEEE Press, Piscataway, NJ, 1994.

[23] P. C. Clemmow, *The Plane Wave Spectrum Representation of Electromagnetic Fields*, Pergamon Press, New York, 1966., Also IEEE Press, Piscataway, NJ, 1996.